Special Issue Processing Design of Single Crystals and Textured Polycrystals for Advanced Electronic Devices

特集

Research Report

Elucidation of the Formation Mechanism of a Textured Ceramic of a P-type Thermoelectric Layered Oxide $[Ca_2CoO_3]_{0.62}[CoO_2]$

Hiroshi Itahara, Won-Seon Seo, Sujeong Lee, Hiroshi Nozaki, Toshihiko Tani, Kunihito Koumoto

P型層状熱電酸化物$[Ca_2CoO_3]_{0.62}[CoO_2]$の配向セラミックス生成メカニズムの解明

板原浩，徐元善，李修妊，野崎洋，谷俊彦，河本邦仁

Abstract

The reactive-templated grain growth (RTGG) method is a powerful fabrication technique for producing textured ceramics having enhanced performance compared to those of conventionally prepared non-textured ceramics, for various functional materials. Its wide applicability is demonstrated by the fact that the RTGG method using β-$Co(OH)_2$ templates gave textured ceramics of p-type thermoelectric layered cobaltites having various compositions. The orientation degree of a prepared ceramic, which influences its performance, depends on the composition of the ceramic. Thus, in order to determine general guidelines for the production of a highly textured ceramic, we analyzed the formation mechanism of the model system $[Ca_2CoO_3]_{0.62}[CoO_2]$ (CCO: Ca_2CoO_3 layer + CoO_2 layer) ceramic on β-$Co(OH)_2$ templates by using high-temperature X-ray diffraction (XRD), pole figure, scanning electron microscopy (SEM) and transmission electron microscopy (TEM). We demonstrated that a textured CCO ceramic is formed through a series of *in-situ* topotactic conversions via intermediate phases with a preserved CoO_2 layer of β-$Co(OH)_2$ templates. In general, we showed, for the first time, that 'a reaction design with partially preserved crystallographic similarities' is essential for the fabrication scheme of a highly textured ceramic with enhanced performance.

Keywords: Formation mechanism of textured ceramics, Reactive-templated grain growth, RTGG, Topotaxy, Reaction design, Layered thermoelectric oxides

要　旨

反応性テンプレート粒成長（RTGG）法は，物性が結晶方位に依存する様々な機能性材料において，無配向セラミックスを凌駕する特性を示す配向セラミックス作製を実現する有力手法である。その有用性は，β-$Co(OH)_2$テンプレートを用いた，各種組成のp型層状熱電コバルト酸化物の配向セラミックス作製例に顕著に示されている。一方，作製するセラミックスの組成により，特性に影響する配向度が異なることが報告されていた。そこで，高配向セラミックスの作製指針を示すために，我々はβ-$Co(OH)_2$と反応補完物質$CaCO_3$とから$[Ca_2CoO_3]_{0.62}[CoO_2]$（CCO：$Ca_2CoO_3$層＋$CoO_2$層）が生成する系をモデルとし，高温XRD，極点図，SEM，TEMにより，その配向継承メカニズムを解析した。その結果，中間相を経由する反応過程において，β-$Co(OH)_2$テンプレートのCoO_2層を維持する一連のトポタクティック変換により，配向CCOセラミックスが生成されることがわかった。より一般的には，配向セラミック・プロセスにおいて，「結晶構造の類似性の少なくとも一部分を継承させる」反応設計が，高特性を発現する高配向セラミックス作製に不可欠であることを，初めて明らかにした。

キーワード：配向セラミックス生成メカニズム，反応性テンプレート粒成長法，RTGG法，トポタキシー，反応設計，層状熱電酸化物

特集

1. Introduction

1. 1 Fabrication techniques of a textured ceramic

The oriented consolidation of anisotropic particles (OCAP) method,[1-3] the templated grain growth (TGG) method[4-7] and the reactive-templated grain growth (RTGG) method[8, 9] have been developed for fabricating textured ceramics. These methods give various functional ceramics with enhanced mechanical (*e.g.* fracture toughness and bending strength) and physical (*e.g.* thermoelectric, piezoelectric, ferroelectric and magnetic) properties compared with conventionally prepared non-textured ceramics. To further enhance these properties, the effect of various process parameters of these methods on the orientation degree of prepared ceramics was investigated by experimental[10, 11] and computational approaches.[12, 13]

The OCAP and TGG methods use single crystalline particles with anisotropic shape (plate-like or needle-like) and include a process stage in which the particles are aligned parallel to one another. These methods require, however, single crystalline particles having target compositions, which limits the material systems for which they can be used. The RTGG method overcomes this disadvantage; this method gave textured ceramics for a variety of compositions.[8, 9, 14-25] We extended the fabrication strategy used in the topotactic synthesis of a textured Mn-Zn ferrite ceramic.[26] In the RTGG method, an anisotropic shaped template particle, which has a different composition but a similar crystal structure to the target ceramic material is used. The template particles are mixed with complementary reactants and aligned parallel to each other. The templates react with the reactants on heat treatment eventually to give textured ceramics.

1. 2 Significance of the formation mechanism of a textured ceramic

Table 1 gives typical examples of RTGG-processed ceramics. First, the textured ceramic of $Bi_{0.5}(Na, K)_{0.5}TiO_3$ (simple perovskite structure) formed on $Bi_4Ti_3O_{12}$ (layered perovskite) templates was reported.[8, 27] Then, recent reports on the fabrication of textured ceramics of $[Ca_2CoO_3]_{0.62}[CoO_2]$[23] (abbreviated to CCO: Ca_2CoO_3 (rock salt-type) layer + CoO_2 layer) and $[Bi_2Sr_{2-x}O_4]_p[CoO_2]$[24] on β-$Co(OH)_2$ templates demonstrated the wide applicability of the RTGG method, *i.e.*, even if a reactive template has only a partial similarity with the crystal structure of the target substance (only the CoO_2 layer is common), the RTGG method gives a textured ceramic.

However, it was reported that the orientation degree of the prepared ceramics depends on their compositions (see Table 1). CCO and $[Bi_2Sr_{2-x}O_4]_p[CoO_2]$ ceramics have Lotgering's orientation degrees[28] (F_{LG}) of 1[23] and 0.67,[24] respectively, although both ceramics are formed on β-$Co(OH)_2$ templates. In the case of a perovskite-type material, the F_{LG} value of a $(Pb_{1/2}Bi_{1/2})(Ni_{1/4}Ti_{3/4})O_3$ ceramic was relatively low, F_{LG} = 0.2.[29] In this case, it was considered[29] that the texture development was disturbed by a metastable intermediate phase, which does not share common crystallographic features with the target material. On the other hand, it is known that the orientation degree of prepared ceramics often drastically affects their performance,[11] thus making it important to

Table 1 Examples of RTTG-processed ceramics.

Template (crystal structure)	Target substance (crystal structure)	F_{LG} [1)]	Features of texture development
$Bi_4Ti_3O_{12}$ (layered perovskite)	$Bi_{0.5}(Na,K)_{0.5}TiO_3$ (simple perovskite)	0.9 [Refs. 8, 27]	Direct conversion from layered perovskite into simple perovskite
β-$Co(OH)_2$ (CdI_2-tpye)	$[Bi_2Sr_{2-x}O_4]_p[CoO_2]$ (misfit-layered)	0.67 [Ref. 24]	–
β-$Co(OH)_2$ (CdI_2-tpye)	$[Ca_2CoO_3]_{0.62}[CoO_2]$ (misfit-layered)	1 [Ref. 23]	Newly clarified mechanism of texture development [Ref. 30]<This report>
$Bi_4Ti_3O_{12}$ (layered perovskite)	$(Pb_{1/2}Bi_{1/2})(Ni_{1/4}Ti_{3/4})O$ (simple perovskite)	0.2 [2)] [Ref. 29]	Intermediate phase disturbs texture development [Ref. 29]

1) Lotgering's orientation degree

2) F_{LG} value was 0.5 for the ceramic prepared under the condition that the formation of an intermediate phase was inhibited by a rapid heating technique [Ref. 29].

investigate the texture preservation mechanism for each material system.

Recently, we elucidated, for the first time, the general principle for the RTGG procedure that a highly textured ceramic is prepared when the crystallographic similarities from the template material all the way through to the target material are 'at least partially maintained' during the formation of the ceramic.[30] Here, we report evidence of this principle based on the formation mechanism of a textured CCO ceramic on β-$Co(OH)_2$ templates: *i.e.*, *in-situ* topotactic conversion of (001) β-$Co(OH)_2$ ⟶ {111} Co_3O_4 ⟶ (001) Ca_xCoO_2 ⟶ (001) CCO.

2. Experimental

2. 1 Fabrication procedure of a $[Ca_2CoO_3]_{0.62}[CoO_2]$ ceramic

Figure 1 shows a schematic representation of the RTGG process for the fabrication of a textured CCO ceramic using β-$Co(OH)_2$ platelets[31] (average diameter ~ 0.5 μm; thickness ~ 0.1 μm; (001) plane developed[32]) as reactive templates. The detail of the fabrication procedure and conditions are described elsewhere.[23, 30] The templates were mixed with $CaCO_3$ (complementary reactant), polyvinyl butyral (binder) and di-n-butyl phthalate (plasticizer) in an ethanol-toluene solution. The mixed slurry was tape-cast by a doctor-blade technique, and the obtained sheet was dried in air, cut, and stacked to form a monolithic plate (green compact). The organic compounds in the green compact were burnt out at 673 K in air (dewaxed compact). Finally, the compact was sintered at 1193 K in O_2 with uniaxial pressure.

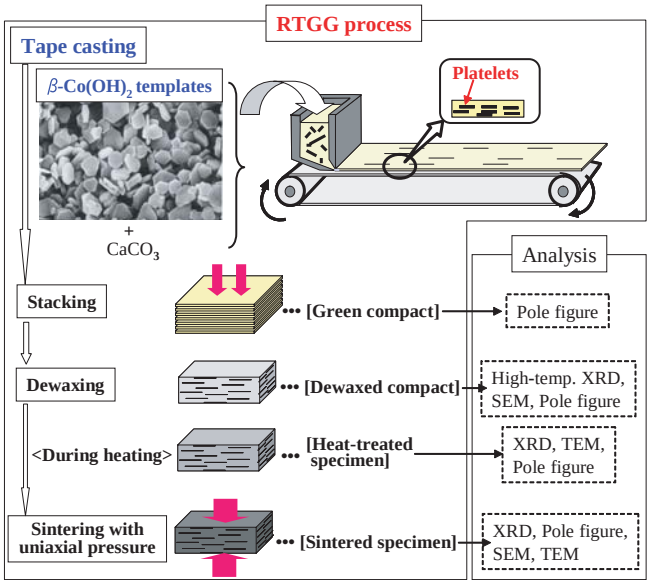

Fig. 1 Schematic representations of the RTGG (reactive-templated grain growth) process using β-$Co(OH)_2$ templates for the fabrication of a textured $[Ca_2CoO_3]_{0.62}[CoO_2]$ (CCO) ceramic[23, 25] and analytical methods used for the elcidation of the formation mechanism of a textured CCO ceramic.

2. 2 Analysis of the formation mechanism of a textured $[Ca_2CoO_3]_{0.62}[CoO_2]$ ceramic

We determined the transition of crystalline phases for the compounds in an RTGG-processed specimen during heat treatment by using high-temperature X-ray diffraction (XRD). The XRD measurement was carried out on a surface parallel to the casting plane of the dewaxed compact after heating in air flow at temperatures of 673, 913, 973, 1103 and 1163 K.

We conducted pole figure (PF) measurements for a green compact, a dewaxed compact, a heat-treated specimen (heated at 973 K in O_2 flow for 10 min) and a sintered ceramic specimen (sintered at 1193 K in O_2 flow for 8 h) in order to determine the preferred orientations of the Co-containing substances produced during processing. We also evaluated the preferred orientation function values[33] for the normal direction to the focused planes of the substances (*e.g.*, (001) plane of β-$Co(OH)_2$).

We observed the microstructure of the heat-treated specimens using a transmission electron microscope (TEM) equipped with EDS in order to confirm that CCO is formed with preserved crystallographic orientations via an intermediate phase formation. In order to observe the microstructural changes that occurred during the formation reaction, the specimens were heat-treated at 1043 K or 1073 K in an O_2 atmosphere with uniaxial pressing at 9.8 MPa for 15 min. For comparison, we acquired TEM and scanning electron microscopy (SEM) images for the sintered ceramic specimen (sintered at 1193 K in an O_2 atmosphere with uniaxial pressing at 19.6 MPa for 20 h), in which the formation of CCO had proceeded to completion.

3. Experimental results and discussion

Figure 2 shows the high-temperature XRD results obtained for the dewaxed specimen, which was found to be a mixture of Co_3O_4 (a decomposed product of β-$Co(OH)_2$ templates) and $CaCO_3$ (Fig. 2 (a)). At 913-973 K, some of the CaO (a product of $CaCO_3$ decomposition) is considered to react with Co_3O_4 to form an intermediate phase (Figs. 2 (b), (c)). The intermediate phase was confirmed[34] to be $Ca_{0.5}[CoO]_2$[35] (hereafter called Ca_xCoO_2) composed of alternating Ca-cation and CoO_2 layers (β-Na_xCoO_2-type Ca_xCoO_2). Ca_xCoO_2 is expected to react with the residual CaO at 1103 - 1163 K to form CCO (Figs. 2 (d)-(e)). It is noted that the prepared CCO ceramic had a (00ℓ) orientation as shown in Fig. 2 (e).

Figure 3 (PF) indicates that the (001), (111), (001) and (002) planes of β-$Co(OH)_2$ in a green compact, Co_3O_4 in a dewaxed specimen, Ca_xCoO_2 in a heat-treated specimen and CCO in a sintered specimen, respectively, were aligned parallel to the casting plane: *i.e.*, these preferred orientations are in the relationship of (001) β-$Co(OH)_2$ // {111} Co_3O_4 // (001) Ca_xCoO_2 // (001) CCO according to the contours concentrated at the pole and the F_{ND} values indicating substantial orientation (F_{ND} = 0.0 for completely random and F_{ND} = 1.0 for perfectly oriented). It should be noted that the four Co-containing substances have a common (or similar) CoO_2 layer in their crystal structure in the direction parallel to the planes listed above. The conversion of the (001) plane of the β-$Co(OH)_2$ templates into the {111} plane of the Co_3O_4 particles was also indicated by SEM observation of the dewaxed compact: *i.e.*, it was found[30] that the Co_3O_4 particles in the compact maintained the morphology of the templates (hexagonal plate-like shape), and that their developed plane was along the casting plane. The relationship for the crystallographic planes of the other substances was confirmed by the obtained TEM images as described below.

Figure 4 (a) indicates that the developed plane of the CCO grains is along the casting plane for the sintered ceramic specimen in which the formation of

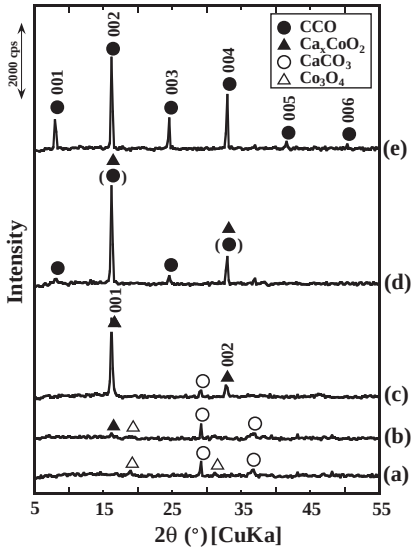

Fig. 2 Results of high-temperature XRD[30] for a surface parallel to the casting plane of a dewaxed compact during heating in air flow: measured at (a) 673 K, (b) 913 K, (c) 973 K, (d) 1103 K and (e) 1163 K: CCO represents $[Ca_2CoO_3]_{0.62}[CoO_2]$.

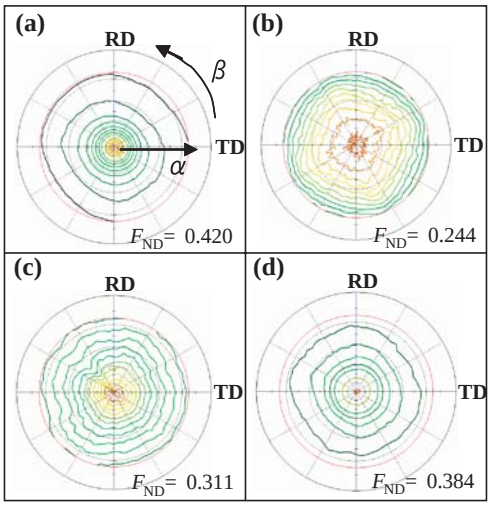

Fig. 3 Results of pole figure measurements[30] for (a) (001) plane of β-$Co(OH)_2$ templates in a green compact, (b) (111) plane of Co_3O_4 in a dewaxed compact, (c) (001) plane of Ca_xCoO_2 in a heat-treated compact (973 K, O_2 flow, 10 min) and (d) (002) plane of CCO ($[Ca_2CoO_3]_{0.62}[CoO_2]$) in a sintered ceramic (1193 K, O_2 flow, 8 h). Azimuthal ($0^o < \beta < 360^o$) scans were carried out in a reflection geometry around the normal direction of the above plane at various polar angles ($0^o < \alpha < 75^o$). F_{ND} represents the value of the preferred orientation function evaluated in the normal direction[33] of the measured plane.

CCO had been completed. The selected area electron diffraction (SAED) pattern agrees that for CCO crystal structure (inset of Fig. 4 (b)). In the high-resolution TEM (HRTEM) image (Fig. 4 (b)), the dark linear contrasts are derived from the CoO_2 layer of CCO while the three arrays of dark spots are due to the triplicate rock salt-type structure of CCO, according to the simulated HRTEM image of CCO (Fig. 4 (c)[36])

Figure 5 represents the cross-sectional HRTEM image of the specimen heat-treated at 1043 K (O_2, uniaxial pressing of 9.8 MPa, 15 min). SAED patterns and fast Fourier transform (FFT) images suggest structural transition from Co_3O_4 (region marked 1) to Ca_xCoO_2 (region marked 2). The FFT image of region 1 (Ca/Co atomic ratio was less than 0.06 by EDS analysis) exhibits a characteristic hexagonal network of reflection intensities for the {111} plane of Co_3O_4 while the FFT image of region 2 (Ca/Co atomic ratio was ~0.4) indicates a layer-structured Ca_xCoO_2. SAED (designated as 3-2) taken from the middle part of the HRTEM image clearly identifies the crystallographic orientation relationship of {111} Co_3O_4 // (001) Ca_xCoO_2, which agrees with the PF shown in Figs. 3 (b), (c).

Figure 6 shows the cross-sectional HRTEM image of the specimen heat-treated at a higher temperature (1073 K) than that for previous specimen in Fig. 5 (heated at 1043 K). In the magnified figure in Fig. 6 (a), three successive dark lines (corresponding to the CoO_2 layer, see Fig. 4 (c)) spaced ~ 0.54 nm apart are gradually transformed into two dark lines aligned at ~ 1.08 nm intervals, with bright and dark contrasts between them. The image on the left hand side is thought to correspond to Ca_xCoO_2 due to the intervals of the adjacent dark linear contrasts (the CoO_2 layer). On the other hand, the image on the right hand side presumably corresponds to a CCO-like structure on the basis of the following results: the spacing of the linear contrasts (the CoO_2 layer) is sufficiently close to those of CCO and the spots due to the rock salt-type layer between the linear contrasts are similar to those of CCO shown in Fig. 4 (b) although they are less evident when compared with those of CCO. The CCO-like structure is considered

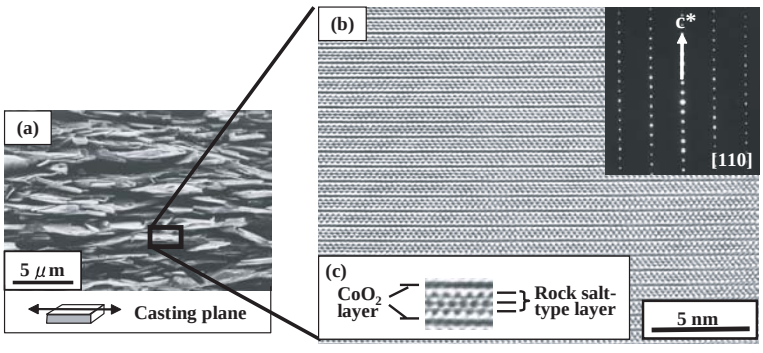

Fig. 4 (a) SEM photograph for a fracture surface perpendicular to the casting plane of a sintered ceramic (1193 K, O_2, uniaxial pressing of 19.6 MPa, 20 h).[30] (b) Cross-section HRTEM image and SAED pattern of the sintered ceramic[30]: the image and diffraction pattern were taken with the incident beam parallel to [110] direction in the unit cell for a Ca_2CoO_3 block of CCO ($[Ca_2CoO_3]_{0.62}[CoO_2]$). (c) The simulated HRTEM image of CCO[36] containing alternating CoO_2 and rock salt-type layers.

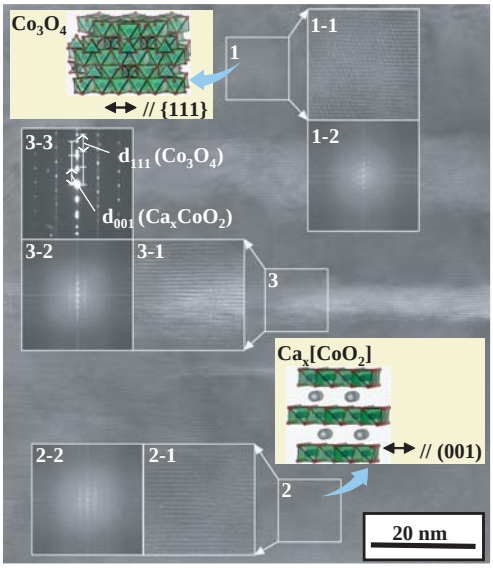

Fig. 5 Fast Fourier transform images (FFTs, No. 1-1, 2-1, and 3-1) of the corresponding cross-sectional HRTEM image[30] (No. 1, 2, and 3) of the heat-treated specimen (1043 K, O_2, uniaxial pressing of 9.8 MPa for 15 min) showed the structural transition from Co_3O_4 (region 1) to Ca_xCoO_2 (region 2). Selected area electron diffraction (No. 3-2) was taken from the middle part, wider region than for FFT filtering, and exhibited the crystallographic orientation relation between Co_3O_4 and Ca_xCoO_2. Insets show the model structures of Co_3O_4 and Ca_xCoO_2.

to be a transient and deficient state during the reaction of CaO (the decomposed product of $CaCO_3$) and Ca_xCoO_2. The previous report[37] supports the appearance of such Ca-deficient CCO before the completion of CCO formation. Thus, a possible interpretation (Fig. 6 (b)) of the observed HRTEM image is that Ca_xCoO_2 provides a part of CoO_2 layers to form the CoO_2 layer of CCO, while the other CoO_2 layers react with Ca and O to form the rock salt-type layer of CCO.

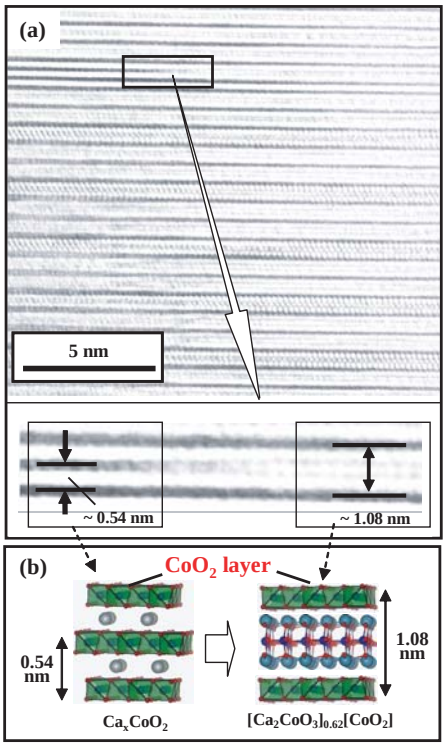

Fig. 6 (a) Cross-section HRTEM image[30] of the heat-treated specimen (1073 K, O_2, uniaxial pressing of 9.8 MPa, 15 min). The image was taken with the incident beam parallel to [110] direction in the unit cell for a Ca_2CoO_3 block of CCO ($[Ca_2CoO_3]_{0.62}[CoO_2]$). (b) The schematic representation of the possible interpretation for the observed contrasts shown in the magnified view for a part of the TEM image.

Figure 7 schematizes the crystal structures of CdI_2-type β-$Co(OH)_2$, spinel-type Co_3O_4 and β-Na_xCoO_2-type Ca_xCoO_2 and misfit-layer-structured CCO. They have common (or similar) CoO_2 layers along the (001) plane in the case of β-$Co(OH)_2$, Ca_xCoO_2 and CCO, and along the {111} plane in the case of Co_3O_4. According to the results described above, it is considered that a series of *in-situ* topotactic conversions of (001) β-$Co(OH)_2$ $\longrightarrow$ {111} Co_3O_4 $\longrightarrow$ (001) Ca_xCoO_2 $\longrightarrow$ (001) CCO is essential for the formation of a textured CCO ceramic on β-$Co(OH)_2$ templates with maintained orientations, where the β-$Co(OH)_2$ template provides the CoO_2 layer.

4. Conclusion

We showed evidence indicating that a textured CCO ceramic is formed in the RTGG process by the *in-situ* topotactic conversion of (001) β-$Co(OH)_2$ $\longrightarrow$ {111} Co_3O_4 $\longrightarrow$ (001)Ca_xCoO_2 $\longrightarrow$ (001) CCO, where β-$Co(OH)_2$ templates provide the CoO_2 layer of CCO via Co_3O_4 and Ca_xCoO_2. In general, the evidence suggests a guiding principle that crystallographic similarities must be 'at least partially maintained' for all materials produced during the processes for the production of a highly textured ceramic.

The RTGG process also provided a textured ceramic of n-type thermoelectric layered oxide $(ZnO)_mIn_2O_3(Z_mIO)$ by using $ZnSO_4 \cdot 3Zn(OH)_2$ platelets as a reactive template.[38-40] In addition,

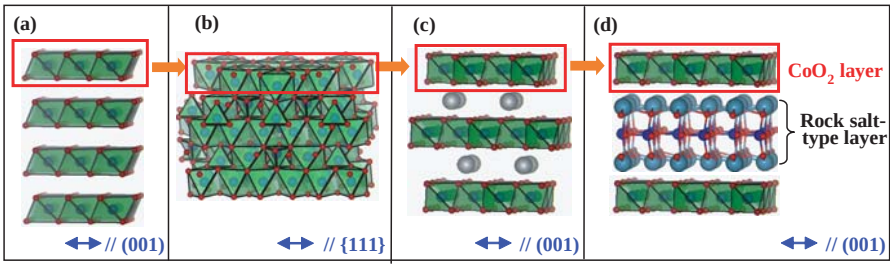

Fig. 7 Schematic representations for the crystal structures of (a) CdI_2-type β-$Co(OH)_2$, (b) spinel-type Co_3O_4, (c) β-Na_xCoO_2-type Ca_xCoO_2 and (d) misfit-layer-structured $[Ca_2CoO_3]_{0.62}[CoO_2]$ (CCO). They are in topotaxial relationship with one another.

R. Asahi et al. demonstrated that the thermoelectric module using RTGG-prepared textured ceramics of p-type CCO and n-type Z_mIO stably generated electric power in a high temperature air atmosphere.[41, 42] We expect that the RTGG process combined with an adequate fabrication scheme of textured ceramics be further applied to the production of not only thermoelectric ceramics but also the other functional ceramics having enhanced performance.

Acknowledgments

We thank Dr. Y. Miyazaki of Tohoku University for giving us structural information on $Ca_{0.5}[CoO_2]$. Drs. K. Horibuchi, Y. Seno, J. Sugiyama, R. Asahi and C. Xia of Toyota CRDL contributed to this work through useful discussions.

References

1) Granahan, M., Holmes, M., Schulze, W. A. and Newnham, R. E. : J. Am. Ceram. Soc., **64**(1981), C68
2) Kimura, T., Holmes, M. and Newnham, R. E. : J. Am. Ceram. Soc., **65**(1982), 223
3) Watanabe, H., Kimura, T. and Yamaguchi, T. : J. Am. Ceram. Soc., **72**(1989), 289
4) Hirao, K., Ohashi, M., Brito, M. E. and Kanzaki, S. : J. Am. Ceram. Soc., **78**(1995), 1687
5) Seabaugh, M. M., Kerscht, I. H. and Messing, G. L. : J. Am. Ceram. Soc., **80**(1997), 1181
6) Hong, S. -H. and Messing, G. L. : J. Am. Ceram. Soc., **82**(1999), 867
7) Sabolsky, E. M., Messing, G. L. and Trolier-McKinstry, S. : J. Am. Ceram. Soc., **84**(2001), 2507
8) Tani, T. : J. Korean Phys. Soc., **32**(1998), S1217
9) Tani, T. : R&D Review of Toyota CRDL (in Japanese), **36**-3(2001), 19
10) Suvaci, E. and Messing, G. L. : J. Am. Ceram. Soc., **83**(2000), 2041
11) Itahara, H., Sugiyama, J. and Tani, T. : Jpn. J. Appl. Phys., **43**(2004), 5134
12) Itahara, H., Nomura, H., Tani, T. and Matsubara, H. : J. Ceram. Soc. Jpn., **111**(2003), 548
13) Itahara, H., Tani T., Nomura, H. and Matsubara, H. : J. Am. Ceram. Soc., **89**-5(2006), 1557
14) Masuda, Y., Nagahama, D., Itahara, H., Tani, T., Seo, W. -S. and Koumoto, K. : J. Mater. Chem., **13**(2003), 1094
15) Itahara, H., Fujita, K., Sugiyama, J., Nakamura, K. and Tani, T. : J. Ceram. Soc. Jpn., **111**(2003), 227
16) Takeuchi, T., Tani, T. and Saito, Y. : Jpn. J. Appl. Phys., **38**(1999), 5553
17) Tani, T., Takeuchi, T. and Seno, Y. : Ceram. Trans., **104**(2000), 267
18) Fukuchi, E., Kimura, T., Tani, T., Takeuch, T. and Saito, Y. : J. Am. Ceram. Soc., **85**(2002), 1461
19) Tani, T., Isobe, S., Seo, W. -S. and Koumoto, K. : J. Mater. Chem., **11**(2001), 2324
20) Tajima, S., Tani, T., Isobe, S. and Koumoto, K. : Mater. Sci. Eng. B, **86**(2001), 20
21) Sugawara, T., Nomura, Y., Kimura, T. and Tani, T. : J. Ceram. Soc. Jpn., **109**(2001), 897
22) Takeuchi, T. and Tani, T. : J. Ceram. Soc. Jpn., **110**(2002), 232
23) Tani, T., Itahara, H., Xia, C. and Sugiyama, J. : J. Mater. Chem., **13**(2003), 1865
24) Itahara, H., Xia, C., Sugiyama, J. and Tani, T. : J. Mater. Chem., **14**(2004), 61
25) Itahara, H. and Tani, T. : R&D Review of Toyota CRDL, **39**-1(2004), 63
26) Hirota, E., Kugimiya, K. and Nishio, T. : J. Jpn. Soc. Powder and Powder Metall., **26**(1979), 123
27) Seno, Y. and Tani, T. : Ferroelectrics, **224**(1999), 365
28) Lotgering, F. K. : J. Inorg. Nucl. Chem., **9**(1959), 113
29) Takeushi, T. and Tani, T. : Key Eng. Mater., **216**(2002), 3
30) Itahara, H., Seo, W.-S., Lee, S., Nozaki, H., Tani, T. and Koumoto, K. : J. Am. Chem. Soc., **127**(2005), 6367
31) Itahara, H., Tajima, S. and Tani, T. : J. Ceram. Soc. Jpn., **110**(2002), 1048
32) Xia, C., Itahara, H., Tajima, S. and Tani, T. : J. Ceram. Soc. Jpn., **112**(2004) S73
33) Hermans, P. H. and Platzek, P. : Kolloid-Z, **88**(1939), 68
34) We determined the crystal structure of Ca_xCoO_2 by conducting Rietveld analysis on the XRD pattern of the heat-treated specimen. For the analysis, we used the crystallographic data of Ca_xCoO_2, which Dr. Y. Miyazaki (Tohoku Univ.) et al. have determined by using a single crystal. The detail of the analysis is described in Ref. 30.
35) Cushing, B. L. and Wiley, J. B. : J. Solid State Chem., **141**(1998), 385
36) Seo, W. -S., Lee, S., Lee, Y., Lee, M. -H., Masuda, Y. and Koumoto, K. : J. Electron Microscopy, **53**(2004), 397
37) Itahara, H., Seo, W. -S., Lee, S., Nozaki, H., Tani, T. and Koumoto, K. : the supporting information of Ref. 30 (see, http://pubs.acs.org)
38) Tani, T., Isobe, S., Seo, W. -S. and Koumoto, K. : J. Mater. Chem., **11**(2001), 2324
39) Isobe, S., Tani, T., Masuda, Y., Seo W. -S. and Koumoto K. : Jpn. J. Appl. Phys., **41**(2002), 731
40) Kaga, H., Asahi, R. and Tani, T. : Jpn. J Appl. Phys., **43**(2004), 7133
41) Asahi, R., Itahara, H., Kaga, H., Okuda, K. and Tani, T. : Proc. 22nd Int. Conf. Thermoelectrics (ICT2004), (2004), 58, IEEE, Piscataway, NJ
42) Asahi, R., Tani, T., Itahara, H., Kaga, H. and Okuda, K. : Proc. 23rd Int. Conf. Thermoelectrics (ICT2005), (2005), 355, IEEE, Piscataway, NJ

(Report received on Mar. 15, 2006)

特集

Hiroshi Itahara
Research fields : Synthesis of thermoelectric materials
Academic degree : Dr. Eng.
Academic society : Ceram. Soc. Jpn., Soc. Chem. Eng., Jpn., Jpn. Soc. Appl. Phys., Chem. Soc. Jpn., Am. Chem. Soc.

Won-Seon Seo*
Research fields : Microstructure analysis by HRTEM, Basic research for ceramic materials, The development of thermoelectric materials
Academic degree : Dr. Eng.
Academic society : Ceram. Soc. Jpn., Korean Soc. Electron. Microscopy, Korean Ceram. Soc., American Ceram. Soc.

Sujeong Lee*
Research fields : Clay mineralogy, TEM study of the phase transformations of ceramic raw materials
Academic degree : Dr. Sci.
Academic society : Korean Soc. Electron. Microscopy, Korea Soc. Economic and Environ. Geology, Korean Ceram. Soc., Clay Miner. Soc.

Hiroshi Nozaki
Research fields : Crystal structure analysis using X-ray and neutron
Academic degree : Dr. Eng.
Academic society : Phys. Soc. Jpn., Jpn. Inst. Met., Jpn. Soc. Synchrotron Radiation Res., Jpn. Soc. Neutron Sci.

Toshihiko Tani
Research fields : Synthesis and texture engineering of functional ceramics
Academic degree : Ph. D.
Academic society : Ceram. Soc. Jpn., Am. Ceram. Soc., Jpn. Soc. Appl. Phys., Jpn. Soc. Powder Powder Metallurg., Mater. Res. Soc. of Jpn.
Award : Jpn. Soc. Powder Powder Metallurg. Award for Innovatory Res., 2002
Ceram. Soc. of Jpn. Award for Academic Achievements, 2005
Dr. Tani concurrently serves as a professor of Toyota Technological Institute.

Kunihito Koumoto**
Research fields : Oxide thermoelectrics, Nature-guided materials processing
Academic degree : Dr. Eng.
Academic society : Ceram. Soc. Jpn., Am. Ceram. Soc., Chem. Soc. Jpn., Am. Chem. Soc., Jpn. Soc. Appl. Phys., Thermoelectrics Soc. Jpn., Int. Thermoelectric Soc., AAAS, Jpn Soc. Inorganic Mater., Jpn. Soc. Powder Powder Metall., Surf. Sci. Soc. Jpn.
Award : Fellow of the Am. Ceram. Soc., 2005
Chinese Ceram. Soc. Award, 2005
Ceram. Soc. of Jpn. Award, 2000
Richard M. Fulrath Award, 1993
President of the Int. Thermoelec. Soc., 2003-2005
Chairman of the Asian Electroceram. Assoc., 2005-2006

*Korea Inst. of Ceram. Eng. and Technol.
**Nagoya Univ.